Routing LEO satellite traffic in adverse weather

Laszlo Toka*ac, Zoltan Illesa, Endre Angelus Pappab, Laszlo Hevizib, Istvan Godorb

Abstract

This research investigates the planning and optimization of sixth-generation (6G) non-terrestrial networks (NTNs) by leveraging Free-Space Optical (FSO) communication to enhance speed, coverage, and resilience in global communication. Building on the theoretical foundation of NTN technologies, this study develops a dynamic simulation model to represent interactions among satellites, ground stations, and environmental variables. Our model allows detailed analysis of weather-induced disruptions, revealing that conditions such as rain and fog can significantly impact radio and FSO-based communication by reducing network speed and reliability. Simulation results show that integrating FSO links alongside traditional microwave connections enhances network adaptability, reducing latency and hop counts, particularly in high-traffic scenarios. In stress tests simulating ground station outages, the network demonstrated resilience by dynamically rerouting traffic over inter-orbit inter-satellite links, maintaining continuity even under significant regional disruptions. These findings underscore the importance of hybrid connectivity models and adaptive routing strategies in 6G NTN planning, providing critical insights for designing robust, high-performance networks capable of meeting future connectivity demands.

Keywords: 6G, satellite, low earth orbit, ground station, precipitation, optimization, inter-satellite, free-space optics

1. Introduction

The emergence of 6G signals a new era in wireless communication; most projections point towards 2030 or beyond for its full-scale deployment. 6G is expected to enhance the capabilities of current networks by leveraging advancements in telecommunication technology: it aims to push the limits of speed, data capacity, coverage and latency to unprecedented levels. Differentiating itself from its predecessor, 6G ventures into higher frequency bands and wider range of bandwidths within the 30 to 300 GHz millimeter waves and is committed to provide enhanced coverage and reliability by combining Terrestrial Networks (TNs) with Non-Terrestrial Networks (NTNs) [1, 2, 3].

The authors of this paper are affiliated with the "6G for Connected Sky" (6G-Sky) project [4] which endeavors to devise comprehensive solutions facilitating dependable and resilient connectivity for both aerial and ground users. This objective is pursued through the implementation of a versatile and adaptive network architecture that integrates various technologies, including satellite and direct air-to-ground communication (DA2GC). Furthermore, the project centers on the development of innovative wireless network design and man-

Preprint submitted to Elsevier

agement schemes within three-dimensional (3D) spatial context. This encompasses the diverse array of flying vehicles, each presenting distinct requirements.

NTNs encompass wireless communication systems that operate beyond the confines of the Earth's surface, employing various platforms such as satellites positioned in low Earth orbit (LEO), medium Earth orbit (MEO), and geostationary orbit (GEO). Additionally, NTNs may involve high-altitude platforms (HAPS) and drones, collectively constituting a diverse array of technological solutions that transcend terrestrial boundaries to facilitate communication and data transmission. Anticipated developments in wireless coverage indicate a transformative shift from traditional 2D 'population coverage' limited to ground surfaces to an expansive 3D paradigm, encompassing 'global and airspace coverage'.

Authors of [5] provide a detailed overview on satellite communication use cases and technologies. Although a wide range of applications are on their list, we only focus on one of the first monetizing segment of use cases, namely on serving global connectivity to aerial users and platforms. We expect that enhanced Mobile Broadband (eMBB) service to airline passengers [6] will initially constitute the bulk of aerial communications. In-flight entertainment may include on-line gaming and extended reality (XR) applications, and both of those heavily rely on low-latency connections. Terrestrial 6G networks intend to support latency below 1 ms under con-

November 5, 2024

^aBudapest University of Technology and Economics, Budapest, Hungary

^bEricsson, Budapest, Hungary

^cAITIA, Budapest, Hungary

^{*}Laszlo Toka (Corresponding author) (email: toka.laszlo@vik.bme.hu).

trolled circumstances [7], while the goal of NTNs is to approach the physically achievable latency limits. Hence primarily LEO communication satellites are planned for deployment by the major providers, moreover Starlink has already applied to FCC for Very Low Earth Orbit (VLEO, altitude of 150-450 km) satellites recently [8].

Our study focuses on providing robust, low-latency, and high-capacity communications using LEO satellite-based NTNs. However, the increasing popularity of these networks raises concerns about congestion in low Earth orbit. The growing number of satellites required for coverage has led to discussions on radio interference, space debris, and collisions, as well as challenges like adverse weather effects, including fog and rain, which can degrade signal quality. Satellite motion, fluctuating traffic demand and adverse weather require dynamic network topology adaptations and advanced management solutions, both of which are central to this research.

The organization of this paper is the following. In Section 2 we discuss the relevant research results in relation with our study. The mathematical model for optimizing network routes through inter-satellite and satellite-ground links taking into considerations weather effects, satellite movement and available communication technologies is introduced in Section 3. Then in Section 4 we present the data that we collected in order to build our findings on real-world input. Afterwards we show the numerical results of the proposed optimization method applied on the collected input data in Section 5. In Section 6 we conclude the paper.

2. Related work

The general satellite communication network may include a combination of LEO, MEO and GEO satellites interconnected by a hierarchical backhaul network and interfaced to terrestrial networks via ground gateways dispersed throughout the continents of Earth. Since most of the satellites are on non-stationary orbit, the traffic demand to a satellite fluctuates in space and time, as do the network topology and link capacities of inter-satellite and satellite-ground connections. As a result, dynamic topology and traffic routing pose major challenges to the management of NTNs and significantly impact the overall NTN performance. [9, 10] present overviews and models of satellite routing algorithms with focusing on the LEO satellite layer. We prefer LEO and VLEO constellations because they are likely to handle the vast majority of mobile broadband traffic (MBB) of remote ground users and airline passengers.

As satellite communications become more affordable due to lower launch and equipment costs, the rapid development of satellite fleets necessitates the use of a large number of inter-satellite links (ISLs) and satellite-ground, also known as feeder links. As a result, mega-constellations of satellites call for more efficient technologies and additional spectrum. The traditional satellite spectrum in the radio frequency (RF) bands (Ku, Ka bands) is becoming a bottleneck for service growth, hence higher operating frequencies with wider band-

widths (Q, V, E bands) and optical spectrum (1550 nm) have been integrated into NTN backbones.

Previously, micro- and millimeter-wave RF spectrum was utilized for feeder links, but the available bandwidth is no longer sufficient, and spectrum utilization is constrained. Millimeter-wave feeder connection technology has progressed, and thanks to widely accepted communication protocols, including DVB-S2X for uplink and DVB-RCS2 for downlink, the offerings for such links are many and diverse. Because radio wave propagation is affected by atmospheric conditions, complex diversification techniques have been developed to improve the dependability and robustness of RF feeder links [11]. We aim to achieve robustness through intersatellite routing and use the ITU models [12, 13] in simulations to address the environment dependency of pathloss.

The authors of [14] performed coincident Starlink and meteorological measurements on user-serving links. They collected and statistically evaluated a half-year long dataset, and their results are also relevant to RF feeder links. The correlation matrices among weather and user traffic measurements, such as throughput, round trip time (RTT), allow to assess the impact of rain and fog on Ku-band satellite-ground links. Mass download of satellite data concerned the authors of [15], who proactively optimized Ka-band satellite-ground links by using weather forecasts and dynamically setting the radio link parameters towards passing weather satellites. Our goals are similar, we also deal with the weather impacts on satellite connections, but we adapt to weather variations by dynamic reconfiguration of the inter-satellite transport network.

Recent developments of millimeter-wave feeder links employ flat, electronically steerable MIMO antennas [16] which can simultaneously maintain connections to a number of satellites without mechanical positioning. Regardless that feeder links in the Q, V and E bands are more sensitivity to rain and other atmospheric components, such feeder links are attractive for the planned satellite mega-constellations [17] thanks to the large bandwidths available in these bands.

Sub-THz (0.1-1 THz) steerable narrow beam antennas would also suit the requirements of inter-satellite communications. Such links [18, 19, 20] can combine the advantage of precision mechanically [21] or electronically steered [21] with MIMO technology and can perform fast pointing, acquisition and tracking at the same time. But technological challenges are yet to be solved, as [19] models the outage probabilities of THz ISL links subjected to the impact of ionosphere plasma, geomagnetic field and pointing errors.

Free-space optical communication (FSO) is a communication technology for air, outer space, vacuum, also suitable to build high-capacity, line of sight (LoS) inter-satellite networks and satellite to ground connections. The main advantage of using laser communications over radio waves is increased bandwidth, it operates in a completely unregulated frequency spectrum resulting in no need for licensing. Additionally, it has low cost on average and it is power efficient. On one side, the narrow invisible beams can communicate 6000 km or further in space and they are fairly difficult to intercept,

on the other hand, beam locking and synchronization between moving transmitter and receiver typically requires mechanical pointing-acquisition-tracking, which may take tens of seconds also causing handover-related outages.

FSO applications include transmitting large amounts of data directly from a satellite, aircraft or unmanned aerial vehicle (UAV) to the ground [22, 23, 24]. Mega-constellations of communication satellites are going to be launched in the coming decade which will demand growing number of ground stations and feeder links [25]. The existing satellite spectrum is limited, interference among feeder links is inevitable, therefore FSO links to ground stations should be applied where the atmospheric conditions are favourable. The most impactful weather phenomena for this technology is fog and rain. Fog is the major factor for the degradation of signal quality since the size of fog particles is nearly the same as the wavelength of a carrier optical signal. This raises an issue, as it modifies light characteristics or completely hinders the passage of light through a combination of absorption, scattering and reflection. Rain is less impactful than the effects of fog because the particles of rain drops are quite big in size compared to the wavelength. Snow and other weather effects have a significantly lower impact on this form of communication. However, different environmental parameters like varying temperature, air refraction index, density and also various pollution particles reduce the visibility and generate adverse effects especially attenuation of optical pulses at different intensity in FSO link and hence degrade the signal quality, making the communication unreliable [26, 27].

A thorough study on atmospheric FSO propagation channel has been provided in [28]. The impact of fog attenuation coefficient, refractive index parameter, coherence length, turbulence model, and angle-of-arrival fluctuation have been modeled for various optical spectral bands.

Corporations like SpaceX, Amazon and OneWeb and a series of startups are currently pursuing various concepts based on laser communication technology. The most promising commercial applications can be found in the interconnection of satellites or high-altitude platforms to build up highperformance optical backbone networks [29]. In conjunction with the Starlink satellite constellation, [30] demonstrate some of the technical challenges lying in the configuration of intersatellite network. Depending on link range, on the orbital relationship between two satellites, the potential connections have different merits and costs, which ISL routing should take into account. [29] models ISL as a hierarchical tiered access network, where the lower tier consists of n satellite mesh routers that serve the UEs, and some of these routers are also gateways to ground stations connecting the ISL to a terrestrial network. The authors start with the traffic flow matrix and they develop a plane sweeping and clustering algorithm that sweeps the network area and captures cluster members one after another under delay and traffic load constraints, which they solve with integer linear programming. Next they describe a greedy edge-appending algorithm, as well as its distributed version, that iteratively inserts edges to maximize algebraic connectivity and form the ISL graph. [31] suggests software-defined networking technique to control ISL routing. A large amount of signaling needs to be exchanged frequently between satellites to dynamically obtain the status information of satellites and ISLs. The status information involves predicted satellite locations, SNRs, link duration and buffer lengths, which are accounted for in a time-variant utility function subjected to optimization. The result of optimization is the time-space evolution of ISL.

[32] investigates a geographical routing scheme in two Walker Star constellations to achieve reliable transmissions with low latency and high data rates. The approach appends a geographical address identifier in Layer 2 of the communication stack such that the globe is thus divided into geographical areas that determine this identifier in the MAC address of the terminals. The MAC addressing scheme is flexible, whereas the IP addresses of the terminals remain static. This decoupling allows for flexibility in the choice of the address resolution scheme by enabling fast routing table lookups and switching. So a robust and adaptable routing scheme is provided for a dynamic environment where satellites and terminals are constantly moving in an Iridium-like constellation.

The authors of [33] approach the ISL routing problem from the aspect of congestion avoidance. They assume steady interconnections among neighbouring satellites and they propose a decentralized congestion avoiding routing mechanism along the established ISLs. Their method seems to pay the price of automatic routing in packet loss and extra packet delay, therefore it should be combined with other ISL topology design methods that predict satellite motion and traffic flows and provisions ISL resources with central control. [34] steps further by performing joint optimization of maximum backhaul capacity and minimum amount of feeder link handovers in a LEO constellation scenario. They define traffic flows along ISLs to ground stations and take into account the time-variant link capacities. Then they formulate the various constraints in the ISL network and solve the system of constraints with mixed-integer programming. Finally they turn the model into a dynamic system, where link and traffic measurements are continuously collected and a central control entity executes on the feeder link handover strategies by running the optimization algorithm periodically.

[35] suggests LEO satellite networks equipped with ISL to provide lower delay compared to traditional optical networks. The inter-satellite routing aims to keep both the power efficiency and end-to-end delay minimal. Their results show that their algorithm outperforms long-haul ISL paths in terms of energy efficiency with only a slight hit to delay performance relative to the conventional ISL topology.

The desired solution to connect megaconstellation of communication satellites to terrestrial networks is to establish sufficient number of diverse ground sites, e.g., by site sharing with terrestrial service providers. However strong satcom players compete for the market and, instead of site sharing, each of them attempts to provide global coverage alone and they chose to minimize the number of central ground sites

to provide sufficient ground capacity at all continents and to backhaul satellite traffic to those sites via ISLs. When a ground site simultaneously carrying connections sometimes to a dozen of satellites is hindered by adverse weather, then reshuffling the inter-satellite backhaul routes may cause service disruptions. Most of the published techniques to combat weather-related impairment of feeder links relies on diversifying ground stations such that nearby ground stations can take each other roles. However, global satcom providers can exploit their continent wide ground station deployments to reroute feeder link traffic from weather impacted sites.

3. Model and routing optimization

The main objective of this research is to optimize the routing of users' Internet traffic in satellite networks based on real-world satellite movement, ground station position and weather data. The task entails mapping ground stations and linking them to satellites with an ever-changing position. Additionally dynamic obstacles posed by weather are introduced to add further realism and complexity. As a result, different network routing scenarios could be compared to observe which could provide the best possible service for customers. The model and optimization method presented in this section can be adapted to any kind of satellite constellation and ground station composition.

3.1. Line of sight

The maximum distance between two satellites that can still see each other, and thus maintain a LoS communication link, depends on several factors, including their altitude and the curvature of the Earth. Most LEO satellites operate at altitudes ranging from approximately 340 km to 1,200 km. For the standard Starlink altitude of about 550 km the distance to the horizon (or the maximum line-of-sight distance to another satellite at the same altitude) is determined by the geometry of the Earth and the satellite's altitude. In the simple calculation one must factor in that the line of sight should also avoid the Thermosphere [36]): $\sqrt{(R_{\text{Earth}} + h)^2 - (R_{\text{Earth}} + t)^2}$, where R_{Earth} is the radius of the Earth (6,371 km), h is the altitude of the satellite (550 km in the case of Starlink), t is the height of Thermosphere, which is typically 80 km. Plugging in the values $\approx 2,500$ km is the distance to the horizon for one Starlink satellite, so the maximum distance between two satellites that can still see each other is roughly 5,000 km.

The line of sight condition provides the ground for establishing edges between nodes in our model, i.e., between aircraft and satellite, satellite and satellite, satellite and ground station. The computed distances between nodes are also important for estimating the transmission latency.

3.2. Rain attenuation

To accurately assess the signal attenuation caused by precipitation and its implications for network efficiency, we used the ITU-Rpy package [12] in this study. This choice was made due to its adherence to ITU-T standards and its provision of a comprehensive framework for calculating attenuation values across a wide range of parameters for frequencies up to 50 GHz. In the context of this study, understanding the level of attenuation induced by rain is important, as severe weather conditions can significantly disrupt network performance, particularly in connections between satellites and ground stations. Rainfall-induced attenuation is influenced by various factors, including the frequency of the transmitted signal, the severity of rainfall, and the altitude and elevation angle of the link.

Frequency plays a significant role in determining the susceptibility of connections to rain attenuation. Higher frequencies are more susceptible to attenuation due to their increased interaction with rain droplets. While lower frequencies may offer greater resistance to rainfall-induced attenuation, they come with lower data throughput capacities. Conversely, higher frequencies enable higher data rates but are more susceptible to attenuation in adverse weather conditions. Consequently, the choice of frequency band for transmission must be carefully considered to mitigate the effects of rainfall.

The severity of rainfall directly impacts the attenuation experienced by connections. Heavy rainfall rates result in greater attenuation, potentially leading to signal degradation or loss. Therefore, accurate characterization of rainfall intensity is essential for predicting network performance during adverse weather conditions.

Additionally, the altitude and elevation angle of the link influence the path length through which the signal traverses the atmosphere. Steeper elevation angles may result in longer atmospheric paths, increasing the likelihood of encountering rain droplets and thus exacerbating attenuation effects. Elevation angles below 15 degrees can result in significant attenuation; however, such extreme angles are rare in practical scenarios due to obstructions caused by natural or man-made obstacles, which typically disrupt line-of-sight connections at such low angles. As elevation angles increase beyond this threshold, the attenuation experienced by the signal decreases gradually. Attenuation tends to level off after reaching approximately 40 degrees, indicating that beyond this point, further increases in elevation angle have minimal impact on reducing attenuation.

In our model media attenuation, e.g. due to rain, fog, etc., degrades the capacity of LoS microwave links according to Shannon's spectral efficiency formula. Let c_0 denote the maximally achievable spectral efficiency on a LoS link in case of free space propagation and let L denote the media attenuation loss ratio that temporarily obstructs the LoS channel. Then due to the extra attenuation the spectral efficiency degrades to

$$c_L(L) = \log_2(1 + (2^{c_0} - 1)L) \tag{1}$$

For $c_0 = 5$ and $c_0 = 6$ (10 and 20 Gbps initial throughput, respectively), the achievable throughput with increasing attenuation is depicted in Figure 1 (L is expressed in dB on the x-axis).

In contrast to the radio links, for the FSO links we implement an on/off switch triggered by weather conditions. If the

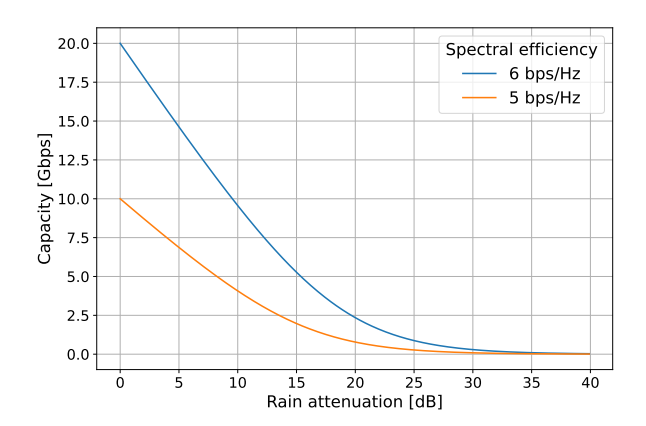


Fig. 1. Degrading capacity due to rain attenuation

attenuation falls below a predetermined threshold, the link remains operational; otherwise, it is temporarily deactivated.

3.3. ILP optimization

Our aim is to optimize the flow of data traffic in a satellite network while minimizing the end-to-end total latency (transmission delay is considered, modulation/demodulation and packet processing delays are omitted). The network comprises users, satellites and ground stations, with specific capacity and latency parameters; we define the following sets and decision variables to represent the network's components and their characteristics accordingly.

Sets

U: Set of users

S: Set of satellites

G: Set of ground stations

Decision variables

 $x_{u,s}$ Binary variable for connection between u and s

 $x_{s,g}^{O}$ Binary variable for connection between s and g using FSO

 $x_{s,g}^{M}$ Binary variable for connection between s and g using microwave

 $x_{s,s'}$ Binary variable for connection between s and s'

 $f_{u,s}$ Flow from user u to satellite s

 $f_{s,g}^{O}$ Flow from satellite s to ground station g using FSO

 $f_{s,g}^{M}$ Flow from satellite s to ground station g using microwave

 $f_{s,s'}$ Flow between satellites s and s'

Objective

Minimize the average transmission latency, i.e., total latency weighted by data traffic flow:

min
$$\sum_{u \in U} \sum_{s \in S} f_{u,s} l_{u,s} + \sum_{s \in S} \sum_{g \in G} f_{s,g} l_{s,g} + \sum_{s,s' \in S, s \neq s'} f_{s,s'} l_{s,s'},$$

where $l_{u,s}, l_{s,s'}, l_{s,g}$ are pre-calculated parameters that represent the distances between user u and satellite s, satellites s and s', satellite s and ground station g, respectively.

Constraints

Flow conservation constraint for each satellite ensuring that the total inflow and outflow of data traffic for each satellite is balanced:

$$\sum_{u \in U} f_{u,s} - \sum_{g \in G} \left(f_{s,g}^{O} + f_{s,g}^{M} \right) + \sum_{s' \in S \setminus s} \left(f_{s',s} - f_{s,s'} \right) = 0 \quad \forall s \in S$$

Minimum outflow constraints for users ensuring that each user u has a minimum required outflow of data:

$$\sum_{s \in S} f_{u,s} \ge d_u \quad \forall u \in U$$

Data traffic capacity constraints for user-satellite links ensuring that the data flow from user u to satellite s does not exceed the capacity of the service link:

$$0 \le f_{u,s} \le c_{u,s} x_{u,s} \quad \forall u \in U, \forall s \in S$$

Data traffic capacity constraints for inter-satellite links ensuring that the data flow from satellite s to satellite s' does not exceed the capacity of the link:

$$0 \le f_{s,s'} \le c_{s,s'} x_{s,s'} \quad \forall s, s' \in S, s \ne s'$$

Data traffic capacity constraints for satellite-ground station links ensuring that the data traffic flow from satellite s to ground station g does not exceed the capacity of the feeder

$$\begin{split} 0 &\leq f_{s,g}^O \leq c_{s,g}^O x_{s,g}^O & \forall s \in S, \forall g \in G \\ 0 &\leq f_{s,g}^M \leq c_{s,g}^M x_{s,g}^M & \forall s \in S, \forall g \in G \end{split}$$

$$0 \le f_{s,g}^M \le c_{s,g}^M x_{s,g}^M \quad \forall s \in S, \forall g \in G$$

Connection limitation constraint ensuring that each user is connected to only 1 satellite, each satellite has connections to at most 4 other satellites, each satellite has a feeder link from only 1 ground station both over microwave and free space optics, and a ground station serves at most 9 satellites with microwave technology.

$$\sum_{s \in S} x_{u,s} \le 1 \quad \forall u \in U$$

$$\sum_{s' \in S \setminus s} x_{s,s'} \le 4 \quad \forall s \in S$$

$$\sum_{g \in G} x_{s,g}^{O} \le 1 \quad \forall s \in S$$

$$\sum_{g \in G} x_{s,g}^{M} \le 1 \quad \forall s \in S$$

$$\sum_{s \in S} x_{s,g}^{M} \le 9 \quad \forall g \in G$$

Adjusting the telescopes for inter-satellite communication can take up to 15-20 seconds, making it inefficient to frequently change the connection structure. Therefore we introduce an extra cost term in the objective function to discourage the number of inter-satellite hops in certain scenarios. The cost function penalizes routing strategies that involve multiple hops. This approach aims to maintain a more stable network configuration, reducing the need for constant realignment of satellite telescopes and minimizing the associated delays and resource usage. By incorporating this cost term, the network can achieve a balance between maintaining latency and reducing the operational overhead associated with frequent telescope adjustments. This ensures that the network operates efficiently, particularly during periods of high demand or when certain ground stations are unavailable.

The penalty term

$$\sum_{s,s'\in S,s\neq s'}p_{s,s'}x_{s,s'}$$

is added to the objective function to penalize inter-satellite connections based on a predefined penalty coefficient. This setup allows the optimization model to account for both the latency and the penalty associated with specific connections, ensuring a more comprehensive optimization that balances efficiency and cost.

4. Input datasets

For our data-driven research we have gathered the satellite, ground station, aircraft and weather data from reliable sources from the internet. We present the gathered datasets in this section.

4.1. Starlink satellites

Satellite movement data, crucial to our optimization method, was sourced from online publications, ensuring accuracy and reliability. This data revealed a comprehensive picture of the current state of Starlink satellites orbiting the Earth. At the time of writing this paper, the dataset encompasses 5811 operational satellites and roughly 900 inactive ones or those that have re-entered the Earth's atmosphere [37]. The

creation of this dataset involved the usage of Python libraries [38, 39] for the precise modeling of satellite orbits, treating them as simple Keplerian ellipses. By incorporating the latest information available about the satellites' current states, including orbital parameters and positional data, the dataset accurately predicts their future locations.

Two-Line Element (TLE) information, available for all satellites, played a pivotal role in this development. TLE data provides detailed orbital elements, enabling precise calculations of satellite positions at specific points in time. Leveraging this information, we can generate a dynamic dataset that captures the movements of satellites over time. Moreover, the time interval between recorded locations can be tailored to meet specific modeling requirements. This adaptability ensures that one can analyze satellite movements with precision and granularity, adjusting the temporal resolution as needed to explore various hypotheses and scenarios.

4.2. Starlink ground stations

The geographical distribution of Starlink ground station locations was determined based on two unofficial online sources [40, 41]. These platforms not only supply users with the geographic coordinates of the establishments but also report detailed insights into the technical specifications of the stations, encompassing parameters such as the number of antennas, uplink and downlink capacities, among others. It is plausible that the release of these technical specifications aligns with regulatory obligations to the Federal Communications Commission (FCC). However, the acquisition of data pertaining to ground stations situated beyond the confines of the United States proves to be notably different.

The absence of official disclosures regarding ground station locations is likely attributable to concerns regarding security. The disclosure of such information could render the infrastructure vulnerable to a spectrum of security threats, including but not limited to malicious attacks and various forms of interference. Such disruptions have the potential to hinder service delivery, resulting in substantial financial losses and eroding customer trust.

An additional aspect of note is the evident discrepancy in the density of ground stations between the United States and other regions, e.g., the 20-30 stations in Europe are depicted in Figure 2. This observation can be explained by the historical context of Starlink's deployment [41]. The initial focus of the provider was on servicing the United States, where the technology was in its emerging stages. Subsequent advancements and refinements in the Starlink satellite network, characterized by the development of a complex routing system between satellites, have obviated the need for a profusion of ground stations to maintain robust and stable connections.

4.3. Air traffic

We have leveraged an air traffic dataset capturing aircraft locations primarily within Europe, with a smaller portion encompassing the Middle East and Africa between September 1 and September 30, 2022. The most important attributes were



Fig. 2. Starlink ground station locations

the latitude and longitude information, essential for spatial analysis, and the icao_actype attribute, which facilitated the matching of scraped passanger capacity information to specific aircraft types. Additionally, a valuable on_ground flag was incorporated into the dataset, offering a helpful filtering criterion. The incorporation of this flag proves necessary, especially considering that ground traffic from airliners is efficiently managed by terrestrial networks, rendering satellite connections unnecessary. By leveraging this on_ground flag, the analysis can selectively focus on relevant data.

4.4. Weather

We used a weather dataset containing hourly data collected from the 26 Starlink ground station locations across Europe. This dataset is sourced from an online platform, enabling free querying, and includes a wide array of meteorological features beneficial for various scientific studies [42]. The dataset's primary significance lies in its relevance to understanding precipitation and cloud cover patterns, particularly in the context of FSO and microwave radio communication systems, which are susceptible to atmospheric disturbances caused by rainfall, fog and cloudiness.

Figure 3 illustrates a notable observation: heavy rainfall events are infrequent occurrences during the month of September. Rainfall disrupts connections at one or more

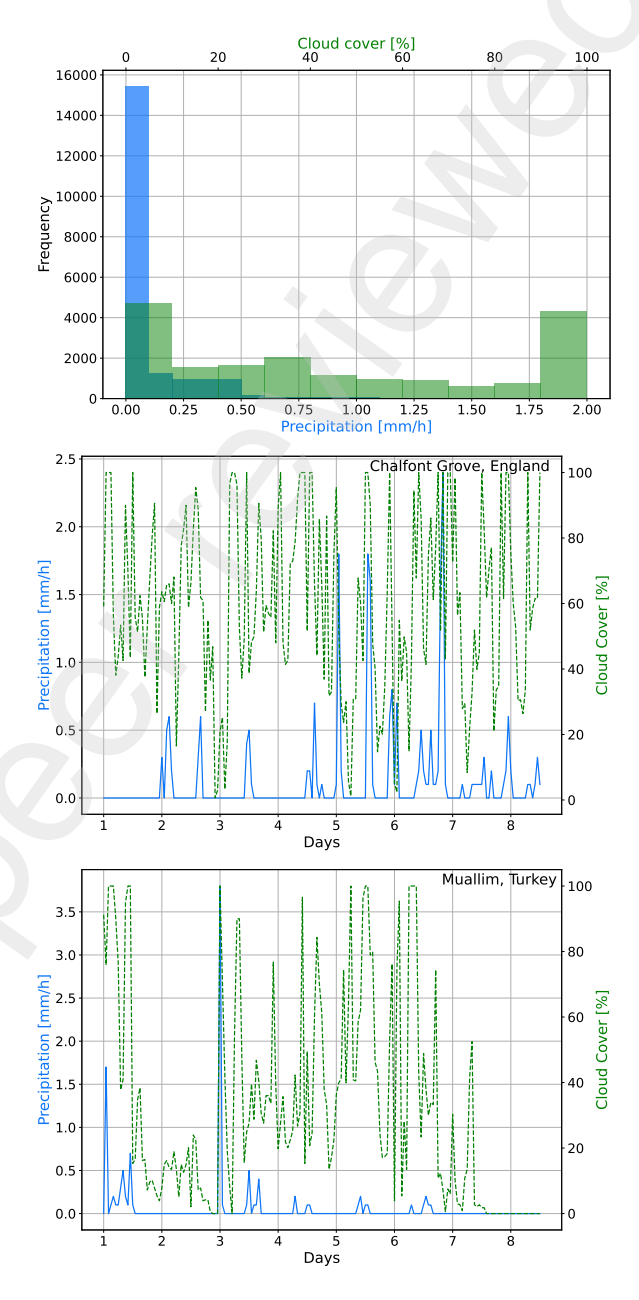


Fig. 3. Rainfall and cloud cover statistics Chalfont Grove and Muallim sites

ground stations approximately 15% of the time, jeopardizing down-link throughput. Weather patterns, particularly rainfall, tend to be spatially coherent, meaning geographically close locations often experience similar conditions. This emphasizes the need for strategic network distribution to prevent simultaneous outages in adjacent areas. A well-spread network can better withstand localized weather disturbances, enhancing system resilience and reducing the risk of widespread outages. Minimizing rain-induced connection disruptions is

essential for maintaining communication network reliability. Proactive weather monitoring, strategic network design, adaptive modulation, and dynamic link management can further mitigate weather-related impacts on feeder links.

5. Numerical results

We have run numerical simulations that offer a dynamic view of how connections between aircraft, satellites, and ground stations adapt over time, factoring in the constant orbital motion of LEO satellites and their shifting positions relative to ground stations. Beyond tracking link changes between satellites and ground stations, the analysis also considers interactions among satellites across various orbits as they periodically enter or exit each other's line of sight.

To thoroughly understand the network's behavior, a multivariable approach that considers a range of metrics in tandem is essential. Such a holistic analysis reveals trends, correlations, and patterns that isolated metrics might overlook. This study is centered exclusively on meeting air traffic demands, with an emphasis on identifying optimal routing strategies based on satellite coverage patterns, user mobility, and realtime weather conditions. These elements are crucial for determining the most efficient data transmission routes within the satellite network.

5.1. Parameter setting

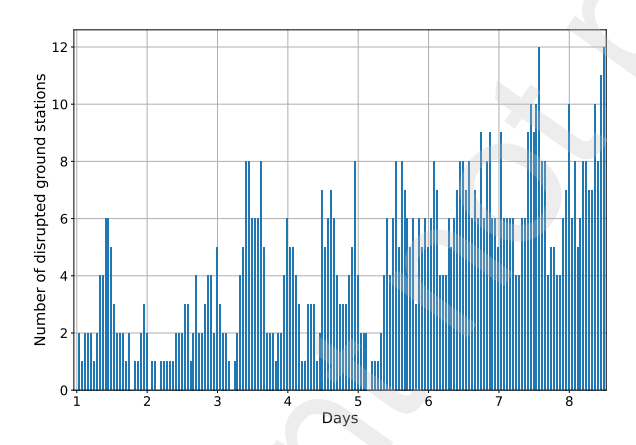


Fig. 4. Number of weather caused disruptions on hourly basis

In this subsection, we outline the key parameters and their values used to simulate the satellite communication network's latency, capacity, and link capabilities. These parameters are essential for modeling realistic communication performance across various links in the network and for assessing the system's resilience under different disruption scenarios. Latency is calculated as the distance between two nodes divided by the speed of light, giving a fundamental measure of transmission delay across each link. Capacity limits vary across different types of connections. For user-to-satellite links, the demand per passenger is set at 5.19 Mbps, based on real-world

data on mobile traffic per subscriber [43, 44]. For satellite-to-satellite connections, link capacity is 20 Gbps due to physical constraints, including satellite payload weight and size limitations. Satellite-to-ground station links vary by technology, with 200 Gbps allocated for Free-Space Optical (FSO) links and 20 Gbps for microwave links, which have a spectral efficiency of 6 bps. Inter-satellite links are limited to a maximum of four connections per satellite based on technical specifications [23].

Table 1 summarizes these key parameters. Disruption levels are analyzed by incorporating various counts of outages within the dataset, providing insights into network resilience under varying levels of operational disruption (Figure 4).

5.2. Transmission delay and inter-satellite hop number results

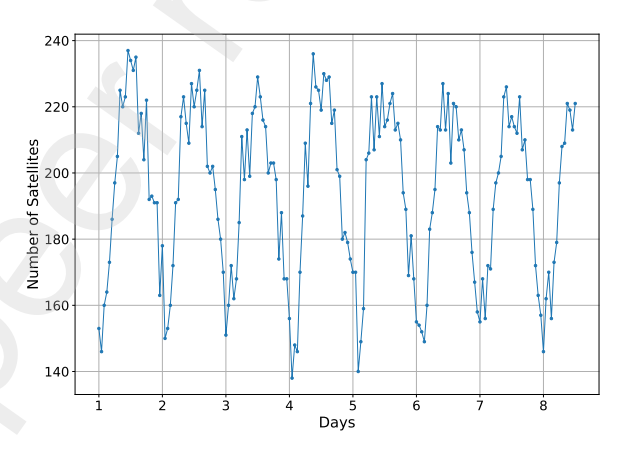


Fig. 5. Number of involved satellites over the simulated time window

A comprehensive analysis of results is key to understanding satellite network performance, as latency alone may not capture all dynamics of data transmission. We therefore aggregate optimization results across time steps, considering satellite movement and air traffic patterns. Our findings reveal that, in certain cases, routing data through multiple satellites yields lower latency than a direct single hop. This is influenced by factors such as user location, ground station distribution, and satellite constellation state, where proximity, line-of-sight availability, and network congestion play a role. Satellite usage trends correlate with daily flight patterns (Figure 5), reflecting capacity limits and bandwidth demand fluctuations in satellite resource allocation. Around midday, when air traffic peaks, satellite usage also rises, showing that resource demand aligns with user distribution and air traffic flow.

Latency Analysis: Most users (75th percentile) experience latency under 10 ms outside of peak hours (Figure 6). Realworld implementations may see higher latency, as switching and buffering dealys are omitted in our model.

Hop Count Trends: The number of hops also follows daily flight trends (Figure 7). During peak times, more hops are often required to manage increased demand. This need

Parameter	Value	Explanation			
	5.19 Mbps	Passenger user demand			
$C_{u,s}$	5 Gbps	Link capacity between aircraft and satellite			
$C_{S,S'}$	20 Gbps	Link capacity between satellites			
$c_{s,g}^{O}$	200 Gbps	FSO link capacity between satellite and ground station			
$\begin{array}{c} c_{s,g}^O \\ c_{s,g}^M \end{array}$	20 Gbps	Microwave link capacity between satellite and ground static			
	6 bps	Spectral efficiency of the microwave link			
$p_{s,s'}$	1	Penalty coefficient for interorbit hops			

Table 1 Parameters used in the simulation.

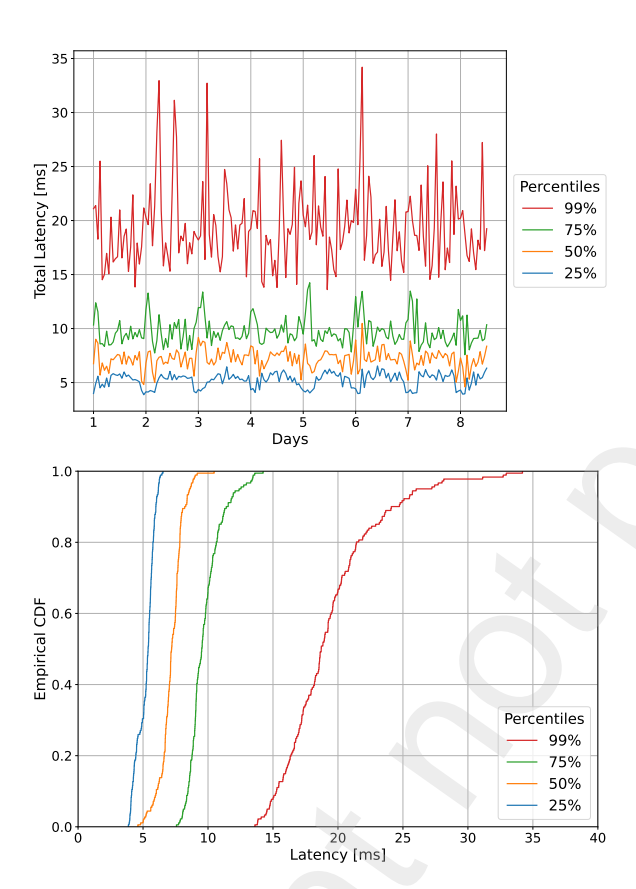
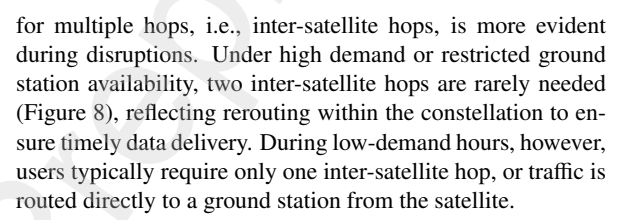


Fig. 6. End-to-end transmission latency statistics over the simulated time window (top) and the empirical cumulative distribution of the latencies of all traffic flow during the the simulated time window (bottom)



Impact of Ground Station Outages: Prolonged outages,

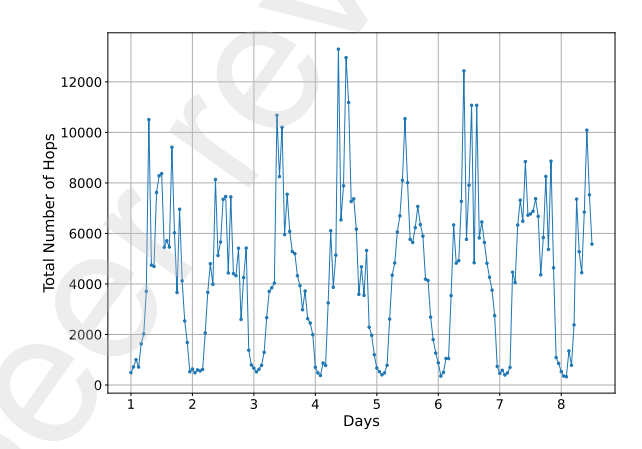


Fig. 7. Number of hops

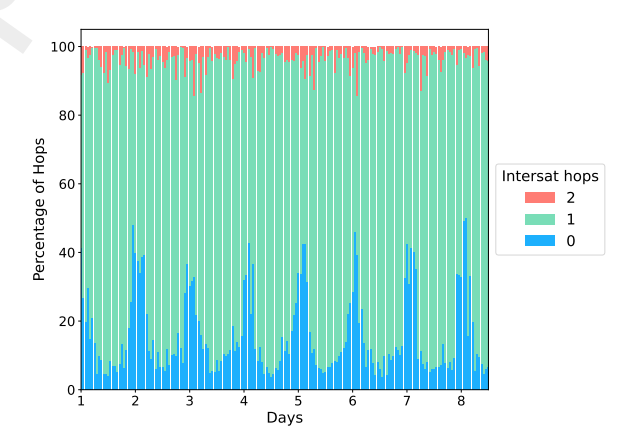


Fig. 8. Hop percentage

such as those caused by rainfall, lead to increased hop counts and longer transmission paths, which raise latency. During such events, the 99th percentile latency rises, impacting data transmission times for many users. While blockages are rare during favorable summer weather, they increase during rainy seasons and have a greater effect when affecting critical or isolated ground stations, as they limit rerouting options. Proximity to other stations can mitigate this impact, while blockages

in isolated or central stations have a pronounced effect on network performance.

5.3. Simulated scenarios

The developed simulation system enables an in-depth analysis of network behavior across several challenging scenarios. Table 2 outlines the parameter settings for the simulated scenarios, each configured to examine network performance under different operational constraints and environmental challenges. These scenarios vary key factors, including the use of Free-Space Optics (FSO) links, limits on microwave connections per ground station, the operational status of UK ground stations, and penalties applied to inter-orbit hops. By adjusting these parameters, the simulations allow for detailed exploration of network behavior under both baseline and stress conditions, revealing how these settings influence the network's capacity to maintain performance amidst disruptions. The FSO and microwave configurations, in particular, highlight potential performance differences in high-demand scenarios and provide insights into how the network might respond to severe outages or limited satellite-ground connectivity.

In the "stress" scenario, all UK ground stations were disabled, simulating a complete regional outage. This drastic reduction in ground station availability—11 stations, or 40% of the total—over an entire week provides insights into the network's response under severe weather conditions. Additional minor outages in other locations were simulated in this scenario, creating a complex environment that tests the resilience of inter-satellite communication, hop counts, and latency patterns as network demand shifts to remaining stations and alternative satellite links.

In scenarios reflecting severe weather conditions, rerouted flights are not modeled due to limited data on potential rerouting paths. Such reroutes would, in reality, redistribute traffic load across the network and affect ground station usage, potentially easing congestion in the affected regions or creating new hotspots. Despite this limitation, the simulations still capture network strain and performance variability under disruptive weather events, allowing for meaningful insights into overall network robustness.

5.4. Comparison of the delay results

The results show distinct network behaviors across the four simulated scenarios compared to the baseline. In the baseline scenario, no FSO communication is used towards ground stations, microwave connections are limited to three per ground station, and UK sites remain operational. Here, inter-orbit hops incur a penalty, making the network avoid such links. This setup results in large hop numbers and latency, limiting network performance with the constrained capacity of traffic routes without inter-satellite connections. The "MW 9" scenario introduces a higher limit of nine microwave connections per ground station, still without FSO links. This increase in microwave connections allows the network to handle more simultaneous connections at each ground station, reducing

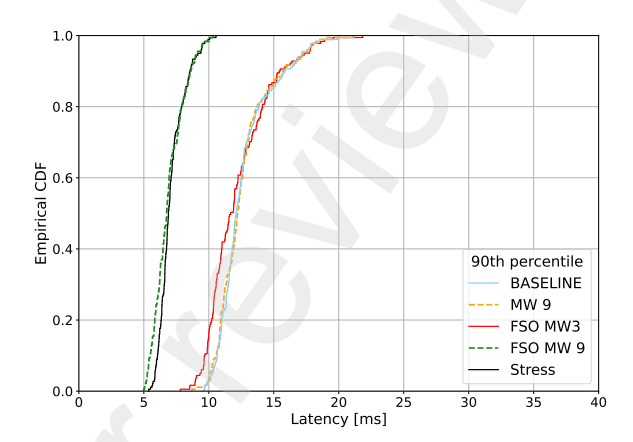


Fig. 9. Comparing 90th percentiles

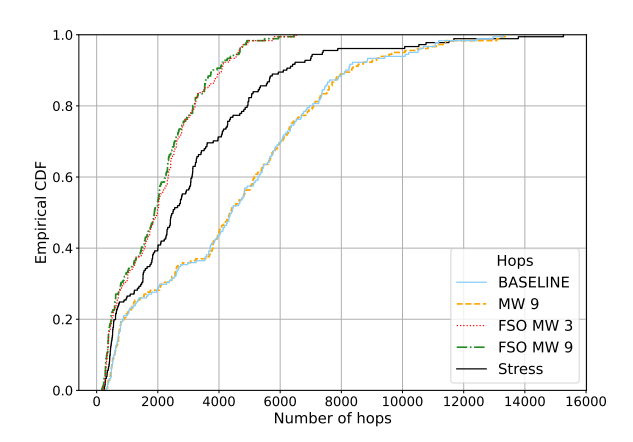


Fig. 10. Comparing number of hops

Parameter	BASELINE	MW 9	FSO MW 3	FSO MW 9	STRESS
FSO feeder link	No	No	Yes	Yes	Yes
Maximum number of microwave connections	3	9	3	9	9
Penalty on inter-orbit inter-satellite links	Yes	Yes	Yes	No	No
UK sites working	Yes	Yes	Yes	Yes	No

Table 2 Simulation parameters of the scenarios

the pressure on inter-satellite links to route traffic. As a result, we would expect a decrease in inter-satellite hop counts (total number of hops is depicted in Figure 10), with more data routed directly between ground stations and satellites, but there is no significant difference compared to the baseline scenario. Therefore this adjustment does not bring down latency either (the empirical distribution of 90th percentile latency of traffic flows is depicted in Figure 9). In this scenario it is apparent that without FSO capabilities, the network's ability to reduce hop counts is limited, suggesting that a hybrid approach with both FSO and microwave connections could offer greater gains in efficiency.

In the "FSO MW 3" and "FSO MW 9" scenarios, FSO communication is enabled, providing high-speed connections between satellites and ground stations. In "FSO MW 3", the microwave connections remain capped at three, while "FSO MW 9" permits up to nine. The FSO links improve network flexibility by reducing inter-satellite hops, enabling shorter paths and less congestion during peak times by minimizing the need for alternate routing paths, demonstrating the effectiveness of both FSO and microwave connections. Compared to the baseline, both FSO scenarios show a more adaptable network structure, with notably fewer delays and fewer hops, especially during midday peaks when traffic is high (hence the depicted 90% percentile in Figure 9). "FSO MW 9" significantly reduces latency not only by allowing a larger volume of connections through each ground station, but also by enabling inter-orbit inter-satellite links.

Finally, the "STRESS" scenario simulates a high-stress network environment with all UK ground stations offline, nine microwave and FSO feeder links per ground station, and no penalties for inter-orbit hops. The loss of UK ground stations forces the network to reroute traffic through alternative paths, significantly increasing the number of hops (Figure 10) and but not affecting latency significantly as data travels through inter-orbit links of the constellation to maintain service (Figure 9). In contrast to baseline conditions, this scenario shows a distinct drop in hop counts, but an extra load on the remaining ground stations, as nearby stations absorb traffic previously handled by the UK sites, shown in Figure 11. This setup illustrates how infrastructure outages, when coupled with high traffic and ample routing options, create manageable stress on the network and result in a tolerable deterioration of latency. This scenario highlights the critical role of infrastructure availability and FSO connectivity in maintaining network resilience under adverse conditions. Analysis of ground station workloads reveals that when a station becomes non-operational, its traffic is absorbed by the nearest available stations, as indicated by the red rings in Figure 11. This redistribution increases the workload of nearby stations: initially, the immediate neighboring stations manage the added load, but once their capacities are reached, excess traffic is progressively routed to stations further away.

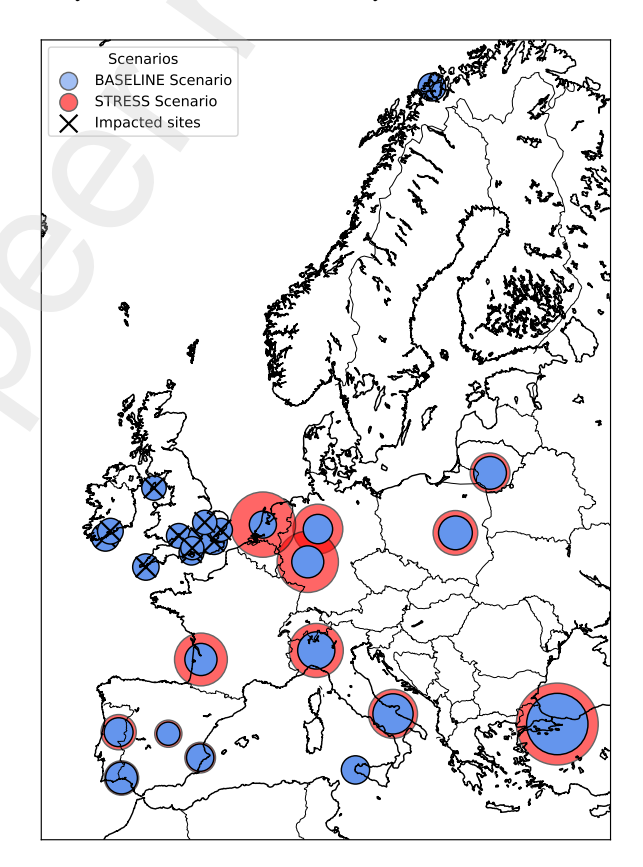


Fig. 11. Workloads in the BASELINE and STRESS scenarios, red highlighting the increased load

In all cases where the policy allows inter-orbit inter-satellite hops, the end-to-end delay of traffic flows show a sizable drop: the 90th percentile of traffic flow latencies is depicted in Figure 9 to demonstrate this effect. The primary reason for this decreased latency is that such links can result in shorter routing paths. Instead of data packets taking the route along satellites in the same orbit, they may travel through shorter paths

via the inter-orbit links. This can reduce delays, especially when the network is under heavy load, such as during midday peaks when user demand is the highest.

5.5. Summary

In scenarios where multiple ground stations experience outages, the ability to dynamically reroute traffic becomes critical. Rigid routing policies that limit the availability of routes can hinder this flexibility, leading to congestion and further latency issues, especially during peak usage periods. Network planners are faced with the challenge of ensuring efficient network performance while also managing operational cost. Enabling the use of inter-orbit inter-satellite hops extends network routing options. This options are enabled in scenarios "FSO MW 9" and "STRESS", and the empirical distribution of the 90th percentile of end-to-end latencies of the routes active at a certain moment shows significantly lower values in these scenarios compared to the others, depicted in Figure 9.

Future advancements in related technologies, such as advanced inter-satellite communication within constellations, improved signal processing techniques, and enhanced spectral efficiency, hold the potential to alleviate capacity constraints and enhance the scalability and flexibility of satellite networks. Predicting the progress is challenging, as it requires consideration of various factors, including not only technological advancements, but also regulatory frameworks, market dynamics, and user demands. While advancements in satellite technology have the potential to address current limitations and expand the capabilities of satellite communication networks, the extent of these improvements will only be realised after widespread adoption within the industry.

6. Summary

This research highlights the transformative potential of satellite networks using Free-Space Optical (FSO) communication as a means to bolster connectivity in next-generation networks, such as 6G. The findings underscore that while 6G's promise of ultra-high-speed, low-latency connectivity marks a significant leap forward, the full realization of its capabilities will require continued advancements in both network infrastructure and technology, particularly in regions where terrestrial networks are limited.

Our simulations and analyses have demonstrated that incorporating FSO technology into satellite networks offers substantial advantages in terms of speed, coverage, and adaptability, particularly in challenging or remote environments. The simulation model developed for this research provides a granular view of user, satellite, and ground station interactions under varying environmental conditions. Findings show that weather-related disruptions, like fog and rain, can significantly impact satellite-to-ground communications, underscoring the necessity of resilient and adaptable configurations in network design. This adaptability is further illustrated in scenarios, where the network effectively maintained continuity

by redistributing loads across alternate pathways, though at the expense of inter-orbit inter-satellite links.

These insights reinforce the importance of hybrid connectivity models that integrate both FSO and traditional microwave technologies. Such configurations offer the dual benefits of network flexibility and enhanced performance, allowing for more direct satellite-to-ground links, minimized latency, and efficient load balancing. The adaptability of satellite routing options, especially in response to air traffic demands and environmental challenges, makes these networks well-suited to future global communication needs.

As research in 6G and satellite technologies progresses, innovations in inter-satellite communication and spectrum efficiency will be vital to scaling these networks. This study contributes to the ongoing discourse on optimal satellite network design, highlighting the critical role of hybrid technologies and flexible routing in ensuring consistent, high-performance global connectivity.

Acknowledgment

This work was supported in part by the CELTIC-NEXT Project, 6G for Connected Sky (6G-SKY), with funding received from the Hungarian National Research, Development and Innovation Office, under the agreement no. 2020-1.2.3-EUREKA-2021-000006.

References

- Sebastian Euler, Xiaotian Fu, Sven Hellsten, Christophe Kefeder, Olof Liberg, Eduardo Medeiros, Erik Nordell, Damanjit Singh, Per Synnergren, Elmar Trojer, Ioannis Xirouchakis, Using 3GPP technology for satellite communication, Ericsson Technology Review (Jun. 2023).
 - URL https://www.ericsson.com/en/reports-andpapers/ericsson-technology-review/articles/ 3gpp-satellite-communication
- [2] Thales Alenia Space France, Ericsson Sweden and Ericsson France, Qualcomm France, SES Techcom, Thales SIX, Telit Cinterion, GreenerWave, Martel Innovate, Digital for Planet, CTTC, German Aerospace Center DLR, Alma Mater Studiorum University of Bologna, Vision on Non-Terrestrial Networks in 6G system (or IMT-2030), in: ETSI Conference, Sophia Antipolis/France, 2024, pp. 1–12.
 - URL https://www.6g-ntn.eu/scientific-publications/
- [3] G. Americas, 5G Americas: Update on 5g non-terrestrial-networks, [Accessed 01-11-2024] (2023).
 URL https://www.5gamericas.org/wp-content/uploads/2023/07/Update-on-5G-Non-terrestrial-Networks-Id.pdf
- [4] 6g for connected sky (6g-sky), [Accessed 01-11-2024] (2022). URL https://www.6g-sky.net/assets/6G-SKY-leaflet-start_hq.pdf
- [5] O. Kodheli, E. Lagunas, N. Maturo, S. K. Sharma, B. Shankar, J. F. M. Montoya, J. C. M. Duncan, D. Spano, S. Chatzinotas, S. Kisseleff, J. Querol, L. Lei, T. X. Vu, G. Goussetis, Satellite Communications in the New Space Era: A Survey and Future Challenges, IEEE Communications Surveys & Tutorials 23 (1) (2021) 70–109. doi:10.1109/COMST.2020.3028247.

- [6] United, The inflight wi-fi revolution now arriving: United signs starlink deal to provide industry-leading connectivity in the sky - for free, [Accessed 01-11-2024] (2024).
 - URL https://www.united.com/en/GB/newsroom/announcements/cision-125346
- [7] 6G mobile network 5G vs 6G network Differences between 5G and 6G network 5G vs 6G technology, [Accessed 01-11-2024] (2024).
 - URL https://www.rantcell.com/how-is-6g-mobilenetwork-different-from-5g.html
- [8] Mark Harris, FCC Denies Starlink Low-Orbit Bid for Lower Latency Agency says SpaceX craft could curb International Space Station operations, IEEE Spectrum (Mar. 2024). URL https://spectrum.ieee.org/starlink-vleobelow-iss
- [9] L. Franck, G. Maral, Routing in networks of intersatellite links, IEEE Transactions on Aerospace and Electronic Systems 38 (3) (2002) 902–917. doi:10.1109/TAES.2002.1039407.
- [10] C. Li, Y. Zhang, Z. Cui, Y. Zhang, J. Liu, Z. Yu, P. Zhang, An Overview Of Low Earth Orbit Satellite Routing Algorithms, in: 2023 International Wireless Communications and Mobile Computing (IWCMC), 2023, pp. 866–870, iSSN: 2376-6506. doi:10.1109/IWCMC58020.2023.10182766.
- [11] T. Rossi, M. De Sanctis, F. Maggio, M. Ruggieri, C. Hibberd, C. Togni, Smart Gateway Diversity Optimization for EHF Satellite Networks, IEEE Transactions on Aerospace and Electronic Systems 56 (1) (2020) 130–141. doi:10.1109/TAES.2019.2917571.
- [12] I. del Portillo, Itu-rpy: A python implementation of the itu-r p. recommendations to compute atmospheric attenuation in slant and horizontal paths., https://github.com/ inigodelportillo/ITU-Rpy/ (2017).
- [13] L. Luini, R. Nebuloni, C. Riva, Ka-to-W Band EM Wave Propagation: Tropospheric Effects and Countermeasures, IntechOpen, Rijeka, 2017, Ch. Section: 3. doi:10.5772/66660. URL https://doi.org/10.5772/66660
- [14] D. Laniewski, E. Lanfer, B. Meijerink, R. van Rijswijk-Deij, N. Aschenbruck, WetLinks: A Large-Scale Longitudinal Starlink Dataset with Contiguous Weather Data, in: 2024 8th Network Traffic Measurement and Analysis Conference (TMA), IEEE, 2024, pp. 1–9. doi:10.23919/tma62044.2024.10558998. URL http://dx.doi.org/10.23919/TMA62044.2024. 10558998
- [15] S. Bellofiore, M. Biscarini, M. Montagna, S. D. Fabio, L. Bernardini, P. Antonelli, P. Scaccia, D. Comite, Weather-Forecast-Driven Satellite Link Optimization: Experimental Validations, IEEE Antennas and Wireless Propagation Letters (2024) 1–5doi:10.1109/LAWP.2024.3404127.
- [16] B. F. Beidas, High-Capacity, Weather-Resilient MIMO Feeder Links in Multibeam Satellite Systems, IEEE Transactions on Communications 70 (7) (2022) 4574–4590. doi:10.1109/TCOMM.2022.3177779.
- [17] Jason Rainbow, SpaceX gets E-band radio waves to boost Starlink broadband, Spacenews (Mar. 2024). URL https://spacenews.com/spacex-gets-e-band-radio-waves-to-boost-starlink-broadband/
- [18] D. Lee, A. Davydov, B. Mondal, G. Xiong, G. Morozov, J. Kim, From sub-Terahertz to Terahertz: challenges and Design Considerations, in: 2020 IEEE Wireless Communications and Networking Conference Workshops (WCNCW), 2020, pp. 1–8. doi:10.1109/WCNCW48565.2020.9124764.
- [19] Y. Li, Y. Chen, Propagation Modeling and Analysis for Terahertz Inter-satellite Communications Using FDTD Methods, in: 2021 IEEE International Conference on Communications Workshops (ICC Workshops), 2021, pp. 1–6, iSSN: 2694-2941. doi:10.1109/ICCWorkshops50388.2021.9473712.

- [20] S. Nie, I. F. Akyildiz, Channel Modeling and Analysis of Inter-Small-Satellite Links in Terahertz Band Space Networks, IEEE Transactions on Communications 69 (12) (2021) 8585–8599. doi:10.1109/TCOMM.2021.3113942.
- [21] Y. Amarasinghe, R. Mendis, R. Shrestha, H. Guerboukha, J. Taiber, M. Koch, D. M. Mittleman, Broadband wide-angle terahertz antenna based on the application of transformation optics to a Luneburg lens, Scientific Reports 11 (1) (2021) 5230. doi:10.1038/s41598-021-84849-8. URL https://doi.org/10.1038/s41598-021-84849-8
- [22] Y. Horst, B. I. Bitachon, L. Kulmer, J. Brun, T. Blatter, J.-M. Conan, A. Montmerle-Bonnefois, J. Montri, B. Sorrente, C. B. Lim, N. Védrenne, D. Matter, L. Pommarel, B. Baeuerle, J. Leuthold, Tbit/s line-rate satellite feeder links enabled by coherent modulation and full-adaptive optics, Light: Science & Applications 12 (1) (2023) 153. doi:10.1038/s41377-023-01201-7.
 - URL https://doi.org/10.1038/s41377-023-01201-7
- [23] Mynaric Laser Communication in Space (2024). URL https://mynaric.com/products/space/
- [24] Terabyte Infrared Delivery 200Gb/sec Laser Communications System for LEO Direct-to-Earth Missions (TBIRD) (2024). URL https://techport.nasa.gov/view/95868
- [25] I. del Portillo, B. G. Cameron, E. F. Crawley, A technical comparison of three low earth orbit satellite constellation systems to provide global broadband, Acta Astronautica 159 (2019) 123–135. doi:10.1016/j.actaastro.2019.03.040. URL https://www.sciencedirect.com/science/ article/pii/S0094576518320368
- [26] S. Borwankar, D. Shah, Effect of Weather Conditions on FSO Link (2020). arXiv:2009.08317.
- [27] K. Dautov, N. Kalikulov, R. C. Kizilirmak, The Impact of Various Weather Conditions on Vertical FSO Links, in: 2017 IEEE 11th International Conference on Application of Information and Communication Technologies (AICT), 2017, pp. 1–4, journal Abbreviation: 2017 IEEE 11th International Conference on Application of Information and Communication Technologies (AICT). doi:10.1109/ICAICT.2017.8687029.
- [28] N. Maharjan, N. Devkota, B. Kim, Atmospheric Effects on Satellite–Ground Free Space Uplink and Downlink Optical Transmissions, Applied Sciences 12 (2022) 10944. doi:10.3390/app122110944.
- [29] I. K. Son, S. Mao, S. K. Das, On the design and optimization of a free space optical access network, Opt. Switch. Netw. 11 (2014) 29-43. URL https://api.semanticscholar.org/CorpusID: 13264254
- [30] A. U. Chaudhry, H. Yanikomeroglu, Laser Intersatellite Links in a Starlink Constellation: A Classification and Analysis, IEEE Vehicular Technology Magazine 16 (2) (2021) 48–56. doi:10.1109/MVT.2021.3063706.
- [31] Z. Han, C. Xu, G. Zhao, S. Wang, K. Cheng, S. Yu, Time-Varying Topology Model for Dynamic Routing in LEO Satellite Constellation Networks, IEEE Transactions on Vehicular Technology 72 (3) (2023) 3440–3454. doi:10.1109/TVT.2022.3217952.
- [32] M. Roth, H. Brandt, H. Bischl, Implementation of a geographical routing scheme for low Earth orbiting satellite constellations using intersatellite links, International Journal of Satellite Communications and Networking 39 (1) (2021) 92–107, _eprint: https://onlinelibrary.wiley.com/doi/pdf/10.1002/sat.1361. doi:https://doi.org/10.1002/sat.1361.
 - URL https://onlinelibrary.wiley.com/doi/abs/10.
 1002/sat.1361
- [33] C.-Y. Chen, Y.-H. Liao, J.-Y. Chen, Congestion Avoid-

- ance Geographic Routing in a Large-Scale Multiple Shell Low Earth Orbit Satellite Constellation, in: 2024 10th International Conference on Applied System Innovation (ICASI), 2024, pp. 383–385, iSSN: 2768-4156. doi:10.1109/ICASI60819.2024.10547783.
- [34] Y. Zhou, J. Liu, R. Zhang, M. Ouyang, T. Huang, A Novel Feeder Link Handover Strategy for Backhaul in LEO Satellite Networks, Sensors 23 (12) (2023). doi:10.3390/s23125448. URL https://www.mdpi.com/1424-8220/23/12/5448
- [35] K. Dakic, C. C. Chan, B. A. Homssi, K. Sithamparanathan, A. Al-Hourani, On Delay Performance in Mega Satellite Networks with Inter-Satellite Links, .eprint: 2307.03881 (2023). URL https://arxiv.org/abs/2307.03881
- [36] D. Bhattacherjee, A. Singla, Network topology design at 27,000 km/hour, in: Proceedings of the 15th International Conference on Emerging Networking Experiments And Technologies, CoNEXT '19, Association for Computing Machinery, New York, NY, USA, 2019, p. 341–354. doi:10.1145/3359989.3365407.
 - URL https://doi.org/10.1145/3359989.3365407
- [37] S. admin@space track.org, Space-Track.org, [Accessed 01-11-2024] (2024). URL https://www.space-track.org/auth/login
- [38] skyfield, [Accessed 01-11-2024] (2024).

- URL https://pypi.org/project/skyfield/
- [39] sgp4, [Accessed 01-11-2024] (2024). URL https://pypi.org/project/sgp4/
- [40] Starlink satellite tracker, [Accessed 01-11-2024] (2024). URL https://satellitemap.space/
- [41] Starlink ground station locations: An overview, [Accessed 01-11-2024] (2024).
 URL https://starlinkinsider.com/starlink-
 - URL https://starlinkinsider.com/starlinkgateway-locations/
- [42] P. Zippenfenig, Open-Meteo.com Weather API, [Accessed 01-11-2024] (2023). doi:10.5281/zenodo.7970649. URL https://open-meteo.com/
- [43] Ericsson, Ericsson Mobility Report, [Accessed 01-11-2024] (2024).
 - URL https://www.ericsson.com/en/reports-and-papers/mobility-report
- [44] Ericsson, Ericsson mobility visualizer mobile data traffic per device per month, [Accessed 01-11-2024] (2024).

 URL https://www.ericsson.com/en/reports-and-papers/mobility-report/mobility-visualizer?f=
 11&ft=1&r=1&t=8&s=1&u=5&y=2023, 2029&c=2